

Zeolites as Transition-Metal-Free Hydrogenation Catalysts: A Theoretical Mechanistic Study

Stefan Senger and Leo Radom*

Contribution from the Research School of Chemistry, Australian National University, Canberra, ACT 0200, Australia

Received September 29, 1999. Revised Manuscript Received December 20, 1999

Abstract: The B3-LYP/6-311+G(3df,2p)//B3-LYP/6-31G(d) procedure has been used to study the zeolite-catalyzed hydrogenation of prototypical doubly bonded systems. Both Brønsted acid and alkali metal sites in model zeolites have been examined. For the hydrogenation of ethene, the barrier is predicted to be lowered by about 50% at the Brønsted acid sites and by about 40% at the alkali metal sites. The barriers for the hydrogenation of formimine and formaldehyde are predicted to be lowered even more substantially, with remarkably low overall barriers of 30 and 60 kJ mol⁻¹, respectively, at the Brønsted acid sites of the zeolites. The alkali metal sites of the zeolites are found to be not quite as effective as the Brønsted acid sites in lowering the hydrogenation barriers in these two cases, as for ethene. Comparisons are made with relevant experimental data.

Introduction

Walling and Bollyky¹ were the first to propose that strong acids catalyze the reaction of molecular hydrogen with unsaturated hydrocarbons. They reported that isobutene and cyclohexene react with hydrogen in the presence of HBr and AlBr₃.² They also found that benzene showed no tendency to do so under similar conditions. By using HF-TaF₅ instead, Siskin³ accomplished the first acid-catalyzed hydrogenation of an aromatic hydrocarbon. The key step in the proposed mechanism is the reaction between the molecular hydrogen and a carbenium ion, which is generated in situ through protonation of a double bond. In the case of benzene, the experimental studies of Wristers⁴ led to the conclusion that the use of an aliphatic solvent is essential for the reaction since the protonated benzene does not react directly with the hydrogen under the experimental conditions. If an aliphatic hydrocarbon, preferably an isoalkane, is present, a hydride transfer occurs from the aliphatic hydrocarbon to the protonated benzene, yielding an aliphatic carbenium ion which subsequently reacts with hydrogen to regenerate the aliphatic hydrocarbon plus the benzene reduction products.

The first theoretical study of acid-catalyzed hydrogenations was undertaken by Bertrán and co-workers⁵ who examined the potential energy surfaces for hydrogenation with ethene as a prototype for an alkene and HF and H₃O⁺ as acids of varying strength. In both cases, the calculated reaction barriers are substantially reduced when compared with the uncatalyzed reaction of ethene with hydrogen; with H₃O⁺ the reaction is almost barrier-free. Although this result looks very promising, Bertrán and co-workers pointed out that a major challenge in finding suitable experimental conditions would be to avoid the addition of the acid to the double bond.

An example of a heterogeneous acid-catalyzed hydrogenation was reported by Sano et al.⁶ In experiments with ethene, they

found that the protonated ZSM-5 zeolite (H-ZSM-5) was active as a hydrogenation catalyst. At a temperature of 818 K, they were able to convert about 95% of the ethene to ethane. Since no metal impurities in the zeolite could be detected, they concluded that the hydrogenation takes place at the acidic sites of the zeolite. These findings give rise to the hope that zeolites could be a useful alternative to the widely used transition-metal-containing hydrogenation catalysts. This is of special interest because hydrogenation reactions are of major importance in the chemical industry. For example, in 1996 at the Swiss-based chemical company Ciba Geigy (now Novartis), more than 90% of catalytic production processes were hydrogenations.⁷

Jacobs and co-workers⁸ performed an extensive study to investigate experimentally the nature of the active sites in zeolites. By varying the reaction temperature and using different types of zeolites with changing Si/Al framework and Na⁺/H⁺ ratios, they reached the conclusion that Na⁺ ions are the active sites at low temperatures and Brønsted acid sites become the active sites if the hydrogenations are performed at higher temperatures. The role of Na⁺ ions as active sites in zeolite-catalyzed hydrogenations had previously been proposed by Minachev et al.⁹

We are unaware of any theoretical studies reported to date on the mechanisms of zeolite-catalyzed hydrogenation reactions. The purpose of the present paper is to try to provide a deeper insight into this type of heterogeneous, catalytic hydrogenation, in which the reaction proceeds without the participation of a transition metal.

As in the experiments of Jacobs and co-workers,⁸ we have chosen ethene as the alkene. Additionally, we include its heteroatom-substituted analogues formimine and formaldehyde in our study to look for systematic trends in behavior. The model

(1) Walling, C.; Bollyky, L. *J. Am. Chem. Soc.* **1961**, *83*, 2968–2969.
(2) Walling, C.; Bollyky, L. *J. Am. Chem. Soc.* **1964**, *86*, 3750–3752.
(3) Siskin, M. *J. Am. Chem. Soc.* **1974**, *96*, 3641–3641.
(4) Wristers, J. *J. Am. Chem. Soc.* **1975**, *97*, 4312–4316.
(5) Siria, J. C.; Duran, M.; Lledós, A.; Bertrán, J. *J. Am. Chem. Soc.* **1987**, *109*, 7623–7629.

(6) Sano, T.; Hagiwara, H.; Okabe, K.; Okado, H.; Saito, K.; Takaya, H. *Sekiyu Gakkaishi* **1986**, *29*, 89–92.
(7) Bader, R. R.; Baumeister, P.; Blaser, H.-U. *Chimia* **1996**, *50*, 99–105.
(8) Kanai, J.; Martens, J. A.; Jacobs, P. A. *J. Catal.* **1992**, *133*, 527–543.
(9) Minachev, Kh. M.; Garanin, V. I.; Kharlamov, V. V.; Isakova, T. A. *Kinet. Katal.* **1972**, *13*, 1101–1112.

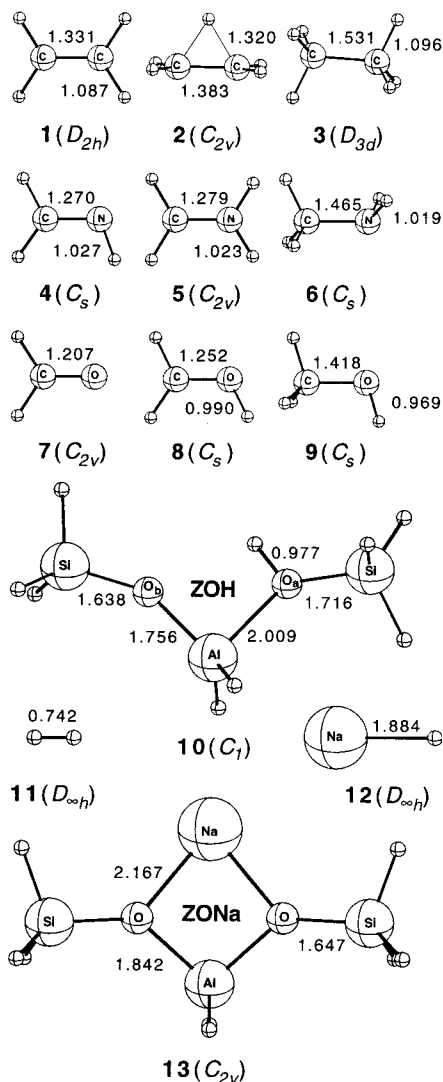


Figure 1. Selected B3-LYP/6-31G(d) bond lengths (Å) for CH_2X , $\text{CH}_2\text{-XH}^+$, CH_3XH ($\text{X} = \text{CH}_2, \text{NH}, \text{O}$), H_2 , NaH , ZOH , and ZONa .

zeolite cluster **10** used in this work, which will be designated ZOH , consists of one aluminum and two silicon tetrahedra whose dangling bonds, which in the authentic zeolite would connect the cluster with the rest of the solid, are saturated with hydrogen atoms: $\text{H}_3\text{Si}-\text{OH}-\text{AlH}_2-\text{O}-\text{SiH}_3$ (cf. Figure 1). To model the Na^+ ions as active sites, the hydrogen atom in the hydroxyl group of this cluster has been substituted by sodium. The resulting cluster ($\text{H}_3\text{Si}-\text{O}-\text{AlH}_2-\text{O}-\text{SiH}_3$) Na (**13**) will be denoted ZONa (also included in Figure 1). The clusters **10** and **13** are considered to represent a reasonable compromise between realistic and computationally affordable models. The sensitivity of the results to cluster size is an important topic for future research.

(10) Hehre, W. J.; Radom, L.; Schleyer, P. v. R.; Pople, J. A. *Ab Initio Molecular Orbital Theory*; Wiley: New York, 1986.

(11) Jensen, F. *Introduction to Computational Chemistry*; Wiley: Chichester, 1998.

(12) Frisch, M. J.; Trucks, G. W.; Schlegel, H. B.; Gill, P. M. W.; Johnson, B. G.; Robb, M. A.; Cheeseman, J. R.; Keith, T.; Petersson, G. A.; Montgomery, J. A.; Raghavachari, K.; Al-Laham, M. A.; Zakrzewski, V. G.; Ortiz, J. V.; Foresman, J. B.; Cioslowski, J.; Stefanov, B. B.; Nanayakkara, A.; Challacombe, M.; Peng, C. Y.; Ayala, P. Y.; Chen, W.; Wong, M. W.; Andres, J. L.; Replogle, E. S.; Gomperts, R.; Martin, R. L.; Fox, D. J.; Binkley, J. S.; Defrees, D. J.; Baker, J.; Stewart, J. P.; Head-Gordon, M.; Gonzalez, C.; Pople, J. A. *Gaussian 94*, Revision E.2; Gaussian Inc.: Pittsburgh, PA, 1995.

Table 1. Calculated B3-LYP/6-31G(d), B3-LYP/6-311+G(3df,2p)//B3-LYP/6-31G(d), and G2^{**} Barriers and Reaction Energies at 0 K (kJ mol^{-1}) for the Uncatalyzed Hydrogenation Reactions

	barrier			reaction energy		
	B3-LYP/ 6-31G(d)	B3-LYP/ 6-311+G (3df,2p)	G2^{**}	B3-LYP/ 6-31G(d)	B3-LYP/ 6-311+G (3df,2p)	G2^{**}
ethene	363	351	363	-142	-123	-125
formimine	348	325	338	-96	-97	-97
formaldehyde	319	289	303	-64	-77	-77

Computational Details

Standard ab initio molecular orbital calculations^{10,11} have been carried out with the GAUSSIAN 94 package of programs.¹² Geometries were generally initially optimized using HF/6-31G(d). In difficult cases, preliminary calculations with the smaller cluster $\text{HO}-\text{AlH}_2-\text{OH}_2$ were performed. Starting from the HF/6-31G(d) geometries, the final optimizations and frequency calculations were carried out with B3-LYP/6-31G(d), and were followed by single-point B3-LYP/6-311+G(3df,2p) energy calculations. Unless otherwise noted, structural parameters in this paper refer to B3-LYP/6-31G(d) values, while relative energies correspond to B3-LYP/6-311+G(3df,2p) values at 0 K, calculated using the B3-LYP/6-31G(d) optimized geometries and incorporating scaled (by 0.9806)¹³ B3-LYP/6-31G(d) zero-point vibrational energy (ZPVE) corrections. For the calculation of the thermal energy and entropy, scaling factors of 0.9989 and 1.0015, respectively, were used.¹³ The intrinsic reaction coordinate (IRC) method was employed to confirm the two minima connected by each transition structure.

Density functional theory (DFT) methods have previously been successfully used to study heterogeneous catalysis in zeolites.¹⁴ Recently, Zygumt et al.¹⁵ tested several DFT methods for studying molecular adsorption in cluster models of zeolites and found that the B3-LYP method showed the best performance. To provide our own benchmark values for comparison, we have used a modified version of G2 , which we will refer to as G2^{**} , to calculate the barriers and reaction energies of the uncatalyzed hydrogenation reactions. G2^{**} employs MP2(fc)/6-31G(d,p) geometries and frequencies (scaled by 0.9608)¹³ rather than the MP2/6-31G(d) and HF/6-31G(d), respectively, of standard G2 .

Results and Discussion

Uncatalyzed Hydrogenation of Ethene, Formimine, and Formaldehyde. The B3-LYP/6-31G(d), B3-LYP/6-311+G(3df,2p)//B3-LYP/6-31G(d), and G2^{**} barriers and reaction energies of the uncatalyzed hydrogenations are grouped together in Table 1 and provide an assessment of the likely quality of the B3-LYP energies for the zeolite-catalyzed hydrogenation reactions. For the barriers, the differences between the B3-LYP/6-31G(d) and G2^{**} values range from 0 (ethene) to +16 kJ mol^{-1} (formaldehyde), whereas all of the B3-LYP/6-311+G(3df,2p)//B3-LYP/6-31G(d) barriers are lower than the G2^{**} values by 12–14 kJ mol^{-1} , that is, the discrepancies in the latter case are more systematic. The differences between the B3-LYP/6-31G(d) and G2^{**} reaction energies range from -17 (ethene) to +13 kJ mol^{-1} (formaldehyde). On the other hand the B3-LYP/6-311+G(3df,2p)//B3-LYP/6-31G(d) reaction energies differ by less than 2 kJ mol^{-1} from the G2^{**} values. These comparisons suggest that the application of B3-LYP/6-311+G(3df,2p)//B3-LYP/6-31G(d) should yield satisfactory results for

(13) Scott, A. P.; Radom, L. *J. Phys. Chem.* **1996**, *100*, 16502–16513.

(14) (a) Nicholas, J. B. *Top. Catal.* **1997**, *4*, 157–171. (b) For a very recent application, see: Saintigny, X.; van Santen, R. A.; Clémendot, S.; Hutschka, F. *J. Catal.* **1999**, *183*, 107–118.

(15) Zygumt, S. A.; Mueller, R. M.; Curtiss, L. A.; Iton, L. E. *J. Mol. Struct. (THEOCHEM)* **1998**, *430*, 9–16.

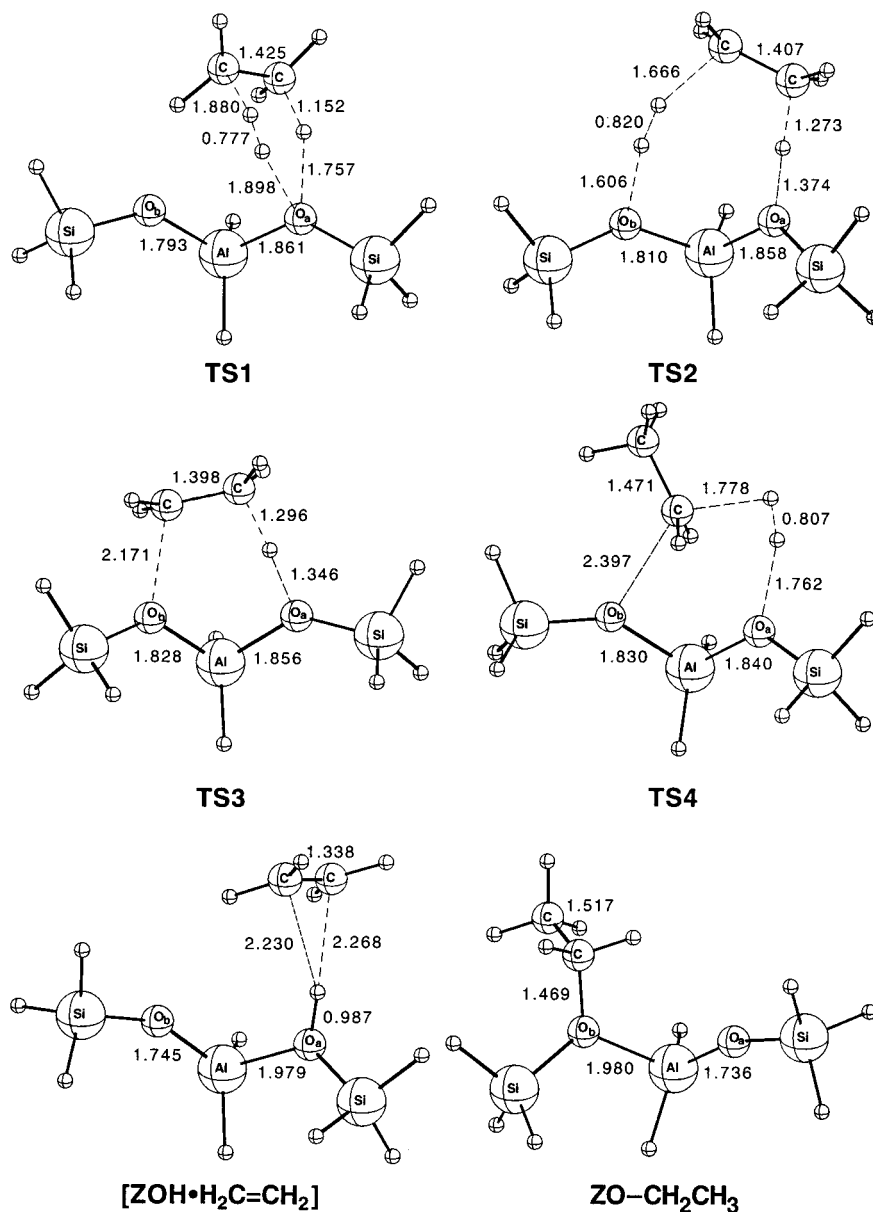


Figure 2. Selected B3-LYP/6-31G(d) bond lengths (Å) for structures relevant to the concerted and stepwise acidic zeolite-catalyzed hydrogenation of ethene.

the zeolite-catalyzed hydrogenation reactions, with errors that are reasonably systematic.

Acidic Zeolite-Catalyzed Hydrogenation of Ethene. By analogy with the transition structures found by Bertrán and co-workers⁵ for the HF- and H₃O⁺-catalyzed hydrogenations of ethene, we initially located a transition structure for the zeolite-catalyzed reaction in which the protonation of the double bond and the cleavage of the H-H bond occur in a concerted manner at a single active site of the zeolite. The resultant structure (**TS1**) is shown in Figure 2. It can be seen that the ethane moiety of this transition structure is partially protonated by the hydroxyl group of the zeolite cluster, the O_a-H bond in the zeolite cluster being lengthened from 0.977 in the model cluster to 1.757 Å, while the H-H bond is extended from 0.742 Å in H₂ to 0.777 Å.

A second transition structure (**TS2**) for a concerted reaction was also located. Whereas in **TS1** a single oxygen atom in the cluster (O_a) acts both as the proton donor and at the same time as acceptor for the proton which is formed upon the heterolytic cleavage of the hydrogen molecule, in **TS2** both oxygen atoms

of the cluster participate in the reaction (see Figure 2). The energy profiles for the concerted mechanisms of the acidic zeolite-catalyzed hydrogenation of ethene via **TS1** and **TS2** are shown in Figure 3a. As can be seen, **TS2** lies 26 kJ mol⁻¹ lower in energy than **TS1**. The barrier for the concerted acidic zeolite-catalyzed hydrogenation of ethene, via **TS2**, is 165 kJ mol⁻¹, which is about half the barrier for the uncatalyzed hydrogenation (351 kJ mol⁻¹ at B3-LYP/6-311+G(3df,2p), Table 1).

We were also able to characterize a two-step reaction pathway for the acidic zeolite-catalyzed hydrogenation of ethene. In the first step, following the formation of a weak complex [ZOH•H₂C=CH₂], ethene is protonated by the zeolite, and an ethoxide (ZO-CH₂CH₃) is formed:



It is well-known that the latter may be formed by the reaction of ethene with acidic zeolites.^{16,17} The transition structure (**TS3**)

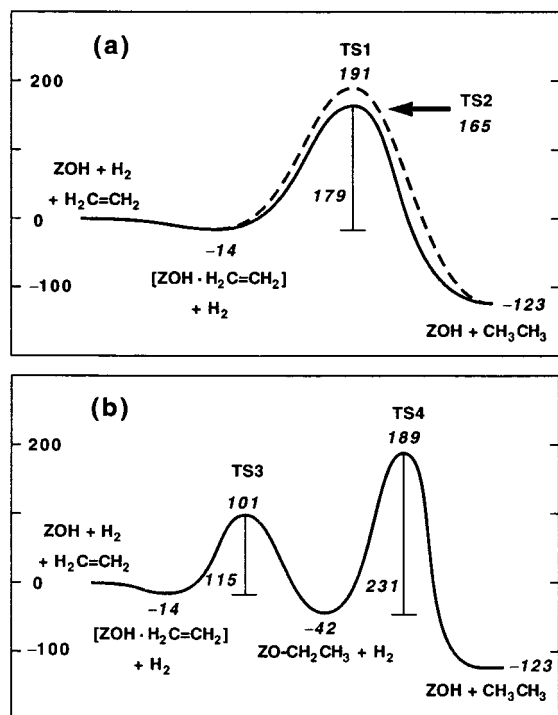


Figure 3. Schematic energy profiles for (a) the concerted and (b) the two-step acidic zeolite-catalyzed hydrogenation of ethene. Relative energies at 0 K are given in kJ mol^{-1} .

for this reaction and the structures of the complex $[\text{ZOH}\cdot\text{H}_2\text{C}=\text{CH}_2]$ and the ethoxide $\text{ZO}-\text{CH}_2\text{CH}_3$ are included in Figure 2.

In the second step, the ethoxide reacts further with hydrogen to form ethane, and the zeolite is regenerated:



For reaction 2 we located the transition structure **TS4** (also included in Figure 2), which has a structure similar to that found by Blaszkowski et al.¹⁸ for the dehydrogenation of ethane, that is, the reverse of reaction 2.

The energy profile for the two-step mechanism of the acidic zeolite-catalyzed hydrogenation of ethene is shown in Figure 3b. Our calculated barrier for step 1 (101 kJ mol^{-1}) is somewhat larger than the 62 kJ mol^{-1} which Evleth et al.¹⁷ obtained at the simpler B-LYP/6-31G(d) level. We find that the second step has a much higher barrier, amounting to 231 kJ mol^{-1} if measured from the ethoxide intermediate, and should be rate-determining. The overall barrier is now reduced to 189 kJ mol^{-1} .

Our calculations predict the concerted mechanism to be energetically favored over the two-step mechanism at 0 K, with a difference in barriers of 24 kJ mol^{-1} . In addition, we find nearly identical values for the standard entropy of activation for the concerted and stepwise mechanisms (B3-LYP/6-31G(d), $T = 298.15 \text{ K}$, $p = 1 \text{ atm}$: $-289 \text{ J mol}^{-1} \text{ K}^{-1}$ (concerted via **TS2**), $-291 \text{ J mol}^{-1} \text{ K}^{-1}$ (stepwise via **TS3** and **TS4**)), suggesting that the concerted mechanism should also be favored at higher temperatures.

Acidic Zeolite-Catalyzed Hydrogenation of Formimine and Formaldehyde. We located transition structures **TS5** and **TS6**, analogous to **TS2**, for the concerted acidic zeolite-catalyzed hydrogenations of formimine and formaldehyde (see Figure 4). IRC calculations confirmed that these transition

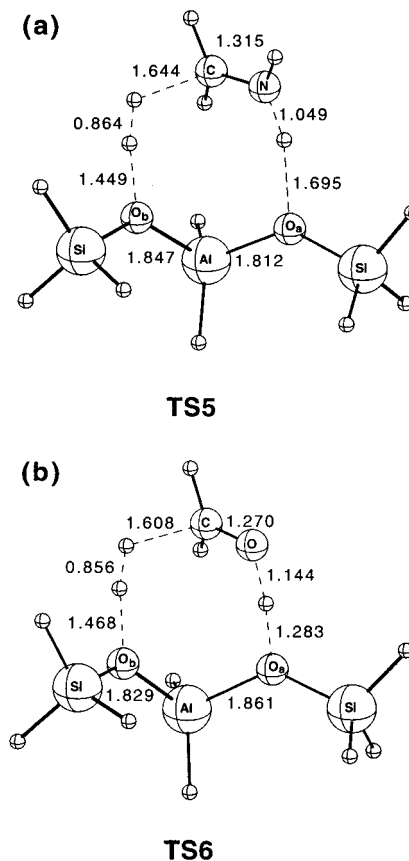


Figure 4. Selected B3-LYP/6-31G(d) bond lengths (\AA) for the transition structures (**TS5** and **TS6**) for the acidic zeolite-catalyzed hydrogenation of (a) formimine and (b) formaldehyde.

structures link reactants that are complexes of formimine/formaldehyde with the acidic zeolite cluster **10** and products that are the corresponding methylamine/methanol complexes (Figure 5). In both transition structures, the O-H bond of the zeolite cluster is substantially lengthened. In the case of the reaction with formimine, the protonation is nearly completed, the bond length of the newly forming N-H bond in **TS5** being 1.049 \AA compared with 1.023 \AA in protonated formimine **5** (cf. Figure 1). On the other hand, the H-H bond of molecular hydrogen has only lengthened from 0.746 to 0.864 \AA . These comparisons show that, although the protonation of the substrate and the cleavage of the molecular hydrogen proceed in a concerted manner, they are not occurring synchronously. In the first phase of the reaction, the substrate is activated through its protonation by the zeolite, while in the second phase the H-H bond is broken heterolytically, the hydride ion component reacting with the protonated substrate and the proton being transferred back to regenerate the zeolite cluster **10**.

While the (concerted) acidic zeolite catalysis of the hydrogenation of ethene reduces the reaction barrier by about 50% (Figure 3a), the catalytic effect is much larger in the case of formimine and formaldehyde (Figure 5). For formimine the barrier is reduced by about 90% from 325 kJ mol^{-1} (uncatalyzed hydrogenation, Table 1) to an overall barrier of only 30 kJ mol^{-1} . For formaldehyde there is a reduction by about 80% from 289 kJ mol^{-1} (uncatalyzed hydrogenation) to 60 kJ mol^{-1} . The ordering of the catalytic effects (ethene < formaldehyde < formimine) correlates smoothly with the proton affinities for the three substrates.

Attempts to locate a transition structure for the hydrogenation of $\text{ZO}-\text{CH}_2\text{NH}_2$ or $\text{ZO}-\text{CH}_2\text{OH}$, that is, the analogues of **TS4**

(17) Evleth, E. M.; Kassab, E.; Jessri, H.; Allavena, M.; Montero, L.; Sierra, L. R. *J. Phys. Chem.* **1996**, *100*, 11368–11374.

(18) Blaszkowski, S. R.; Nascimento, M. A. C.; van Santen, R. A. J. *Phys. Chem.* **1996**, *100*, 3463–3472.

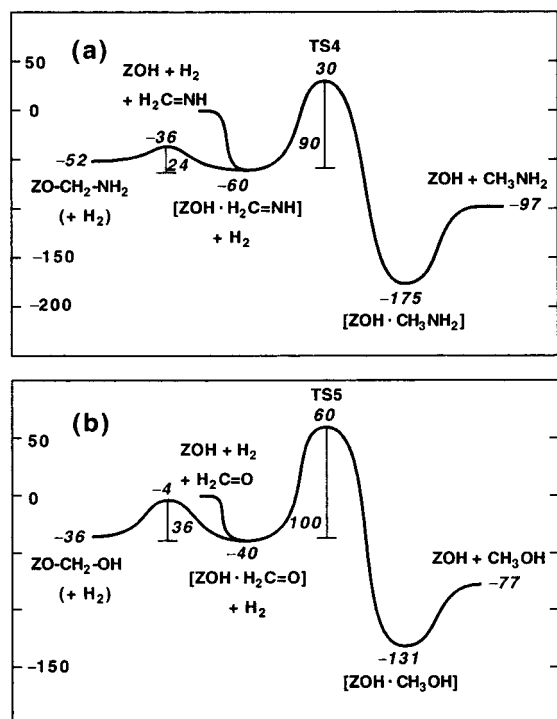


Figure 5. Schematic energy profiles for the acidic zeolite-catalyzed hydrogenation of (a) formimine and (b) formaldehyde. Relative energies at 0 K are given in kJ mol^{-1} .

in reaction 2, were not successful. In all cases the geometry optimizations led to the transition structures **TS5** or **TS6** for the concerted reactions. In this context it is worth mentioning that, in contrast to the situation with ethene, the reactions of the weak complexes of formimine and formaldehyde with the acidic zeolite cluster¹⁹ to form zeolite-bound species (analogous to $\text{ZO}-\text{CH}_2\text{CH}_3$) have very small barriers and are nearly thermoneutral (see Figure 5).

Cationic Zeolite-Catalyzed Hydrogenation of Ethene. Minachev et al.⁹ suggested that in the first step of the catalytic hydrogenation, a heterolytic dissociative adsorption of hydrogen occurs on the cationic forms of zeolites:



On the basis of calculations of thermal effects of the interaction of hydrogen with halides and hydroxides of alkali metals (as simple model systems for cationic zeolites), they came to the conclusion that reaction 3 is exothermic.²⁰ However, our calculations predict that reaction 3 is strongly endothermic, the relative energy of $\text{ZOH} + \text{NaH}$ compared with $\text{ZONa} + \text{H}_2$ being 301 kJ mol^{-1} . Therefore, it is rather unlikely that this reaction plays a significant role in the catalytic process. Nevertheless, we decided to search for the transition structure for reaction 3 and for the resulting complex $[\text{ZOH}\cdot\text{NaH}]$. At the HF/6-31G(d) level of theory, we were able to locate the transition structure for the reaction of molecular hydrogen with the smaller cluster $(\text{HO}-\text{AlH}_2-\text{OH})\text{Na}$ as well as for the complex $[(\text{HO}-\text{AlH}_2-\text{OH}_2)\cdot\text{NaH}]$. However, after the incorporation of ZPVEs, the transition structure is found to lie lower in energy than the complex. With the larger cluster ZONa (**13**), neither the transition structure nor the complex could be located

(19) The structures of $[\text{ZOH}\cdot\text{H}_2\text{C}=\text{NH}]$, $[\text{ZOH}\cdot\text{H}_2\text{C}=\text{O}]$, $\text{ZO}-\text{CH}_2\text{NH}_2$, and $\text{ZO}-\text{CH}_2\text{OH}$ are included in the Supporting Information.

(20) Minachev, Kh. M.; Kharlamov, V. V.; Garanin, V. I. In *Catalysis on Zeolites*; Kalló, D., Minachev, Kh. M., Eds.; Akadémiai Kiadó: Budapest, 1988; pp 489–514.

on the HF/6-31G(d) potential energy surface. Therefore it is most likely that the complex $[\text{ZOH}\cdot\text{NaH}]$ is not a stable species.

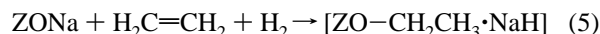
An alternative reaction step could be the reaction analogous to the formation of $\text{ZO}-\text{CH}_2\text{CH}_3$ in the case of the acidic zeolite-catalyzed reaction:



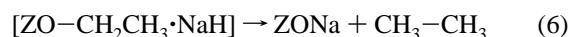
However, as for reaction 3, we were only able to locate the product of reaction 4 for the smaller cluster $(\text{HO}-\text{AlH}_2-\text{OH})-\text{Na}$. On adding two silyl groups to this structure, the subsequent optimization led back to the complex $[\text{ZONa}\cdot\text{H}_2\text{C}=\text{CH}_2]$, so that reaction 4 can also be ruled out as an initial step.

We were, however, successful in locating the transition structure (**TS7**) for a termolecular reaction between ZONa (**13**), ethene, and hydrogen (Figure 6). This bears some resemblance to **TS2** but occurs significantly later on the reaction pathway. In contrast to the acidic zeolite-catalyzed hydrogenation via **TS2**, it is possible in principle to formulate an intermediate species, the complex $[\text{CH}_3\text{CH}_2\text{Na}\cdot\text{ZOH}]$, for the reaction via **TS7**. However, our attempts to locate $[\text{CH}_3\text{CH}_2\text{Na}\cdot\text{ZOH}]$ on the potential energy surface have not been successful (similar to the situation for the complex $[\text{ZOH}\cdot\text{NaH}]$ mentioned above), and there is no indication from the IRC calculations of a stable intermediate on the reaction path from **TS7** to the products, ZONa plus ethane. The energy profile for the reaction is shown in Figure 7a.

We have also found transition structures (**TS8** and **TS9**) corresponding to an alternative two-step process. IRC calculations reveal that **TS8** connects the reactants, ZONa , ethene, and hydrogen, with $[\text{ZO}-\text{CH}_2\text{CH}_3\cdot\text{NaH}]$, a complex between the ethoxide and NaH (see Figure 6), bound with respect to these two components by 55 kJ mol^{-1} :



For the second reaction step the transition structure **TS9** was located, corresponding to the formation of ethane and regeneration of ZONa :



Reaction 6 is similar to reaction 2 (via **TS4**) in the acidic zeolite-catalyzed hydrogenation (Figure 3b), but with H_2 substituted by the much more effective hydrogenation agent NaH . The energy profile for the sequence of reactions 5 and 6 is depicted in Figure 7b.

With an overall barrier of 203 kJ mol^{-1} (and a standard entropy of activation of $-247 \text{ J mol}^{-1} \text{ K}^{-1}$), compared with 259 kJ mol^{-1} (and a slightly larger value for the standard entropy of activation of $-276 \text{ J mol}^{-1} \text{ K}^{-1}$) for the rate-determining first step of the two-step reaction, the concerted reaction via **TS7** (Figure 6a) should be the favored mechanism for the cationic zeolite-catalyzed hydrogenation of ethene, irrespective of the temperature. We use overall barriers rather than the energy differences between the complex $[\text{ZONa}\cdot\text{H}_2\text{C}=\text{CH}_2]$ plus H_2 and the transition structure in these considerations, because $[\text{ZONa}\cdot\text{H}_2\text{C}=\text{CH}_2]$ will not be a stable species at normal temperatures. For example, the standard free energy (i.e., at $T = 298.15 \text{ K}$, $p = 1 \text{ atm}$) for formation of this complex from its components is $+5 \text{ kJ mol}^{-1}$.

Cationic Zeolite-Catalyzed Hydrogenation of 2-Methyl-1-butene: Experimental Comparison. Experimental data show that during the hydrogenation of 2-methyl-2-butene on an RbNaY zeolite, isomerization about the double bond takes

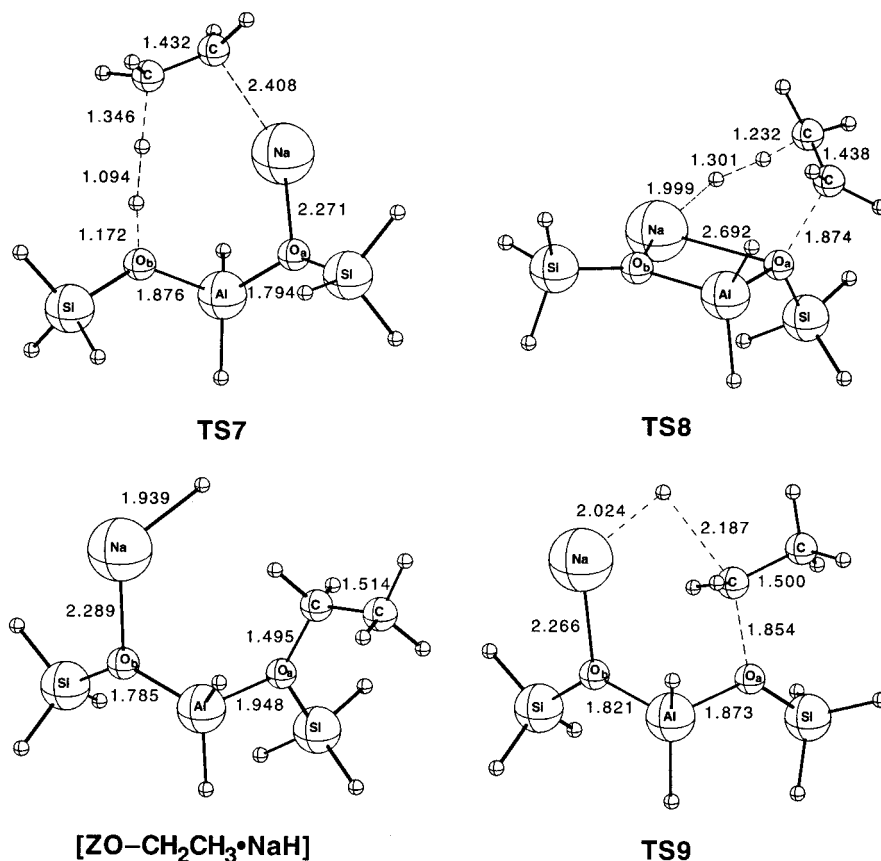


Figure 6. Selected B3-LYP/6-31G(d) bond lengths (Å) relevant to the concerted and stepwise cationic zeolite-catalyzed hydrogenation of ethene.

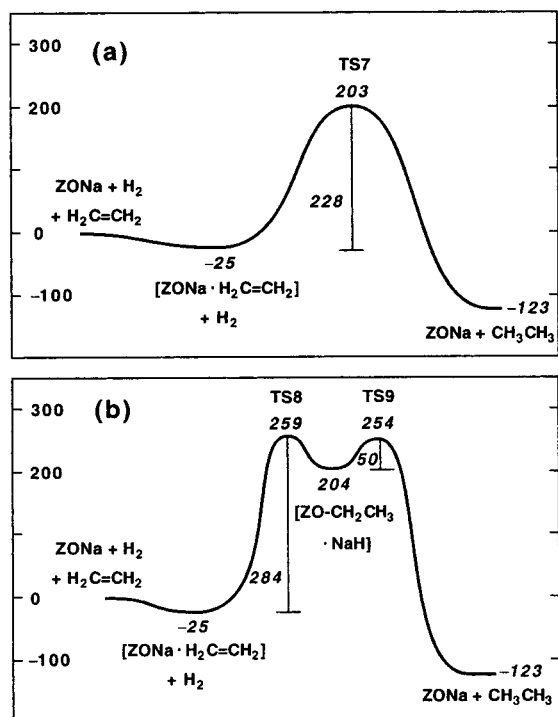


Figure 7. Schematic energy profiles for (a) the concerted and (b) the two-step cationic zeolite-catalyzed hydrogenation of ethene. Relative energies at 0 K are given in kJ mol^{-1} .

place.²¹ Thus, in addition to the isopentane hydrogenation product, 2-methyl-1-butene is produced. This has been interpreted as indicating that molecular hydrogen is adding to the

double bond of the reactant successively as individual atoms or ions.²¹ Our calculations on the cationic zeolite-catalyzed hydrogenation of ethene suggest an isomerization mechanism in which the initial reaction is analogous to reaction 5 (Figure 7b) of the stepwise mechanism. Thus, in the primary step of the reaction of 2-methyl-2-butene ($\text{Me}_2\text{C}=\text{CHMe}$) with ZONa and hydrogen, the complex of $\text{ZO}-\text{CMe}_2\text{CH}_2\text{Me}$ with NaH should be formed.²² This complex can then either react further to form isopentane plus ZONa, or there will be a back reaction to form an alkene again. Depending on whether NaH reacts with a hydrogen from the methylene group or with a hydrogen from one of the α -methyl groups of $[\text{ZO}-\text{CMe}_2\text{CH}_2\text{Me}\cdot\text{NaH}]$, either the reactant 2-methyl-2-butene or its isomer 2-methyl-1-butene will be produced.

We have carried out explicit calculations on the cationic zeolite-catalyzed hydrogenation of 2-methyl-1-butene to examine these possibilities. As can be seen in Figure 8a, the calculated overall barrier (relative to the isolated reactants) for the *isomerization* of 2-methyl-2-butene to 2-methyl-1-butene (in the presence of the cationic zeolite cluster ZONa and hydrogen) at 0 K is 272 kJ mol^{-1} . The reaction involves a conformational isomerization (**I** \rightarrow **II**) of the intermediate complex, $\text{ZO}-\text{CMe}_2-\text{CH}_2\text{Me}\cdot\text{NaH}$. We have not located the transition structure for this conformational transformation but have confirmed through potential energy scans that it is a low-energy process. For the concerted ZONa-catalyzed *hydrogenation* (via a transition structure analogous to **TS7**) of 2-methyl-2-butene (Figure 8b), we calculate a barrier of 258 kJ mol^{-1} . The energy difference between the barriers for the isomerization and the concerted hydrogenation of 2-methyl-2-butene is sufficiently small to

(21) Kharlamov, V. V.; Garanin, V. I.; Tagiev, D. B.; Minachev, Kh. M. *Izv. Akad. Nauk SSSR, Ser. Khim.* **1975**, 2406–2410.

(22) The Markovnikov product, $\text{ZO}-\text{CMe}_2\text{CH}_2\text{Me}$, is likely to be favored over the alternative possibility $\text{ZO}-\text{CHMe}-\text{CHMe}_2$.

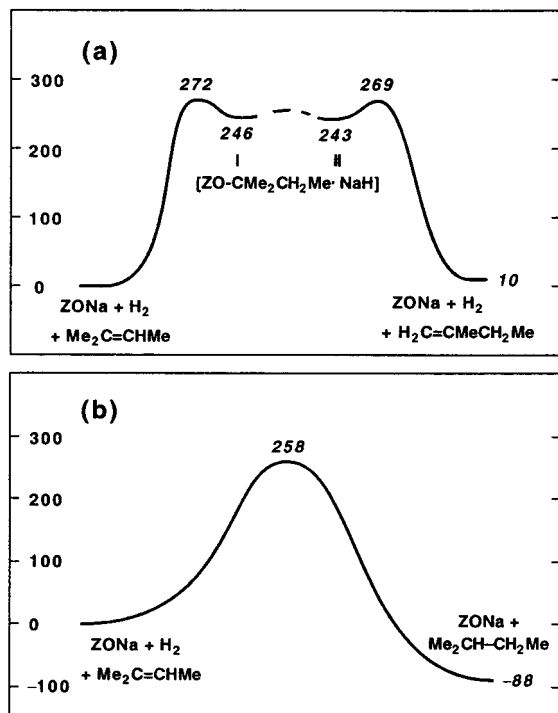


Figure 8. Schematic energy profiles for (a) the cationic zeolite-catalyzed isomerization of 2-methyl-2-butene and (b) the cationic zeolite-catalyzed hydrogenation of 2-methyl-2-butene. Relative energies at 0 K are given in kJ mol^{-1} .

conclude that at least some isomerization should be observed, consistent with the results of the experimental study.

Nature of the Active Site in the Zeolite-Catalyzed Hydrogenation of Ethene. Jacobs and co-workers⁸ concluded that in zeolites which contain alkali metal cations as well as acidic sites, the alkali cations are the active sites at the lower experimental temperature (623 K), whereas the acidic sites are active at the higher temperature (723 K). Our calculations predict that at 0 K the concerted hydrogenation of ethene catalyzed by ZONa (13) has a barrier of 203 kJ mol^{-1} (relative to the isolated reactants, cf. Figure 7a), compared with only 165 kJ mol^{-1} for the (concerted) hydrogenation (TS2) catalyzed by ZOH (10) (cf. Figure 3a). In addition, for the concerted ZONa-catalyzed reaction we calculate a standard entropy of activation (B3-LYP/6-31G(d), $T = 298 \text{ K}$, $p = 1 \text{ atm}$) of $-247 \text{ J mol}^{-1} \text{ K}^{-1}$, while it is $-289 \text{ J mol}^{-1} \text{ K}^{-1}$ for the concerted ZOH-catalyzed reaction (via TS2). This leads to the result that at the lower of the temperatures examined by Jacobs et al.⁸ ($T = 623 \text{ K}$, $p = 20 \text{ atm}$), the difference in the free energies of activation shrinks to 16 kJ mol^{-1} , with calculated values of 331 kJ mol^{-1} (catalyzed by ZONa) and 315 kJ mol^{-1} (catalyzed by ZOH). At the higher temperature (723 K), the calculated values are 351 kJ mol^{-1} (catalyzed by ZONa) and 339 kJ mol^{-1} (catalyzed by ZOH). With such small energy differences, it is not possible to decide definitively on the basis of the calculations which active site is favored. However, our calculations do not appear to offer an immediate explanation for the observed temperature dependence. It is possible that differential adsorption may have an influence.²³

Cationic Zeolite-Catalyzed Hydrogenation of Formimine and Formaldehyde. For the ZONa-catalyzed hydrogenation of formimine and formaldehyde, the transition structures TS10 and TS11 were located. As can be seen in Figure 9, TS10 and TS11 have geometries very similar to those for the corresponding

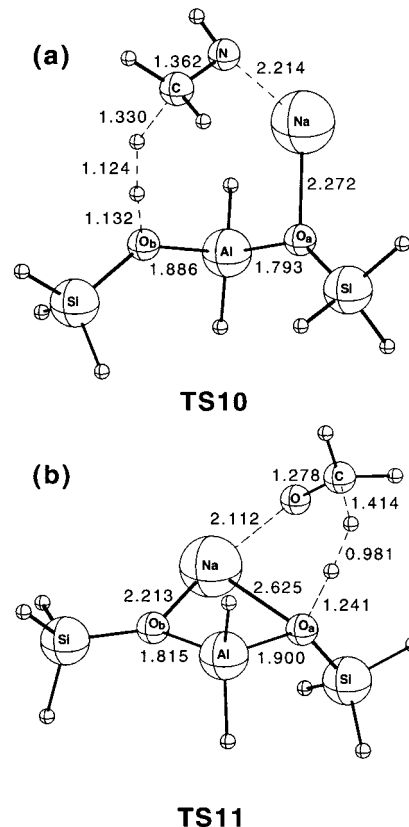


Figure 9. Selected B3-LYP/6-31G(d) bond lengths (\AA) for the transition structures (TS10 and TS11) for the cationic zeolite-catalyzed hydrogenation of (a) formimine and (b) formaldehyde.

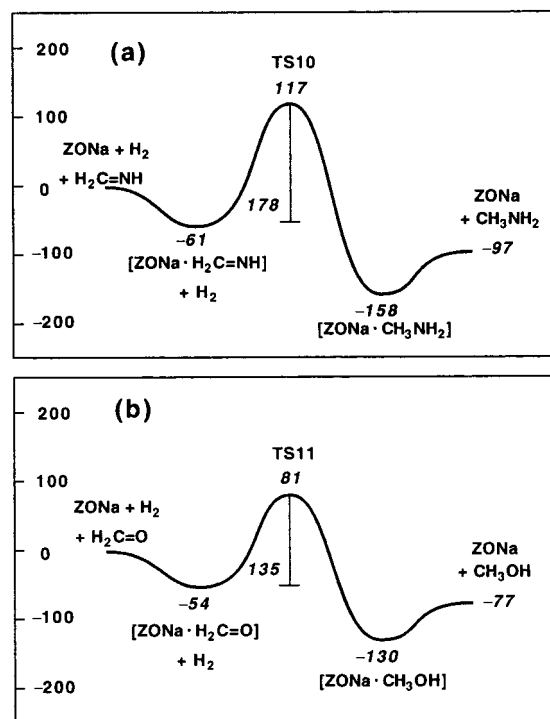


Figure 10. Schematic energy profiles for the cationic zeolite-catalyzed hydrogenation of (a) formimine and (b) formaldehyde. Relative energies at 0 K are given in kJ mol^{-1} .

transition structures (TS5 and TS6) for the acidic zeolite-catalyzed hydrogenations (cf. Figure 4). IRC calculations show that TS10 and TS11 connect the reactant complexes $[\text{ZONa} \cdot \text{H}_2\text{C}=\text{X}]$ ($\text{X} = \text{O}, \text{NH}$) plus H_2 directly to the product complexes

(23) See, for example: van Santen, R. A.; Kramer, G. J. *Chem. Rev.* 1995, 95, 637-660.

[ZONa·CH₃XH] and that no further intermediates are involved in the reactions. With overall barriers of only 117 kJ mol⁻¹ for formimine and 81 kJ mol⁻¹ for formaldehyde (see Figure 10), compared with 325 kJ mol⁻¹ and 289 kJ mol⁻¹ (cf. Table 1) for the uncatalyzed reactions, ZONa has a significant catalytic effect. It is, however, not as large as for the catalysis with the acidic zeolite cluster ZOH.

The only carbonyl compounds whose experimental zeolite-catalyzed hydrogenations have been reported to date are acetone^{24,25} and acetaldehyde.²⁰

Concluding Remarks

In the present investigation, we have applied the B3-LYP/6-311+G(3df,2p)//B3-LYP/6-31G(d) procedure to study the mechanisms of zeolite-catalyzed hydrogenation reactions of prototypical doubly bonded systems at Brønsted acid sites and alkali metal cation sites of the zeolites. Compared with the barrier in the uncatalyzed hydrogenation, the barriers calculated for the (concerted) zeolite-catalyzed hydrogenation of ethene

(24) Minachev, Kh. M.; Garanin, V. I.; Kharlamov, V. V.; Kapustin, M. A. *Izv. Akad. Nauk SSSR, Ser. Khim.* **1974**, 1554–1557.

(25) Minachev, Kh. M.; Garanin, V. I.; Kharlamov, V. V.; Kapustin, M. A. *Izv. Akad. Nauk SSSR, Ser. Khim.* **1975**, 2673–2678.

are reduced by about 50% at the acidic active sites and by about 40% at the cationic active sites. For formimine and formaldehyde, we make the remarkable prediction that the hydrogenations at the Brønsted acid sites proceed with extremely small barriers. With an activation energy of only 30 kJ mol⁻¹, the acidic zeolite-catalyzed hydrogenation of formimine is almost barrier free.

Acknowledgment. We gratefully acknowledge generous allocations of time on the Fujitsu VPP300 and SGI Power Challenge computers of the Australian National University Supercomputing Facility.

Supporting Information Available: GAUSSIAN 94 archive entries for B3-LYP/6-31G(d)-optimized geometries of relevant equilibrium structures and transition structures (Table S1), calculated B3-LYP/6-31G(d) total energies and ZPVEs and B3-LYP/6-311+G(3df,2p)//B3-LYP/6-31G(d) total energies (Table S2), and selected pictorial representations (Figure S1) (PDF). This material is available free of charge via the Internet at <http://pubs.acs.org>.

JA9935097